Progress In Electromagnetics Research C, Vol. 102, 175–185, 2020

Dual-Feed, Dipole Antenna System for 2.4/5.2/5.8-GHz, Tri-Band WLAN Laptop Applications

Che-Chi Wan and Saou-Wen Su*

Abstract—A low-profile, printed dipole antenna having two feed ports with two parasitic strips for tri-band operation in the 2.4 GHz (2400–2484 MHz), 5.2 GHz (5150–5350 MHz), and 5.8 GHz (5725–5825 MHz) wireless local area network (WLAN) bands is presented. The strip dipole is coupled-fed via a chip capacitor connected to a dual-feed network and generates the 2.4 and 5.2 GHz bands with the aid of the tuning stubs in the feed network. The two parasitic strips are further employed to introduce additional resonance to cover the 5.8 GHz band. It was found that by loading the chip capacitor with proper values between the strip dipole and the dual-feed network, the port decoupling in both the 2.4 and 5.2 GHz bands can be improved, making a dual-feed and yet single antenna system possible. The design with constant strip width is simple in structure and occupies a compact size of 5 mm × 40 mm (about 0.04-λ × 0.32-λ at 2.4 GHz), which is well-suited to current narrow-bezel laptop computers.

1. INTRODUCTION

For laptop computers working in heterogeneous wireless networks, more and more antennas for different wireless communications are expected to be incorporated into devices. The laptop computers with the fifth-generation (5G) capability built in can be, for example, equipped with as many as nine antennas, among which seven antennas are used for 5G networks (LTE/sub-6 GHz/millimeter-wave) and two antennas for Wi-Fi/Bluetooth connectivity [1]. With the growing demand for multiple antennas integrated into wireless devices, the available space for antenna designs becomes critically constrained. The size of the antenna and the mutual coupling between the nearby antennas operating in the same frequency band are, accordingly, considered the major issues for antenna engineers.

In conventional design methodology for two closely-paired antenna systems, it is quite common to introduce an additional decoupling structure (resonator) as to provide a new coupling path against the original coupling between two identical antennas for isolation enhancement [2–7]. However, the main drawback is that the use of these decoupling structures limits further reduction in the design footprint because of certain spacing wasted.

Recently, two-antenna systems that require no decoupling structure and show good isolation have been favorably reported [8–12]. The self-isolated antennas in a close-form loop structure when being packed in pairs in close proximity [8] do not need any decoupling structure between the antennas and show isolation better than 17 and 14 dB in the 2.4/5 GHz bands. In [9], two gap-coupled antennas having asymmetrical mirrored structures are shown to exhibit isolation $>$ 10 dB in the 3.4–3.6 GHz band. In [10], two coupled-fed, U-shaped antennas sharing one coupled grounding strip for self-decoupling with isolation $>$ 17 dB in the 3.4–3.6/4.8–5.0 GHz bands are presented. Two resonances are found in the antenna pair. The first resonance is coupled between two antenna elements and not useful, while the second resonance is decoupled using the shared coupled grounding strip [10]. The conjoined coupled-fed

Received 11 April 2020, Accepted 20 May 2020, Scheduled 1 June 2020
* Corresponding author: Saou-Wen Su (Saou-Wen_Su@asus.com).
The authors are with the Antenna Design Department, Advanced EM & Wireless Communication R&D Center, ASUS, Taipei 11259, Taiwan.

loops in [11] with no separation between the two antennas for the 3.3–4.2 GHz band are reported to obtain isolation > 12 dB. The conjoined section embedded with a chip capacitor is reported to act as a band-pass structure, which attracts more currents on the ground excited by one port and suppresses currents entering the other port, thereby decoupling the two antenna ports.

The decoupled two monopoles with two parasitic grounded strips conjoined to achieve isolation better than 19 and 16 dB for 2.4 and 5 GHz operation are introduced in [12]. A chip capacitor is also used but loaded between the conjoined section and the antenna ground. Different from [11], the capacitor allows the conjoined strips to generate two different resonant modes close to each other with out-of-phase currents on one parasitic strip when the other strip is excited. Good decoupling is thereby attained.

Despite no decoupling structure [8–10] or even no antenna separation of the conjoined designs [11, 12], the above-mentioned designs in [2–12] are still based on two discrete antenna elements. In this paper, we demonstrate that a single radiator (one antenna element) can be fed by two signal ports, which are decoupled using the same radiator, and yet function as a two-antenna system. The design comprises a simple strip dipole, a dual-feed network, and two parasitic strips. The strip dipole is coupled-fed via a chip capacitor connected to a dual-feed network and generates 0.5-, 1.0-, and 1.5-λ dipole modes. The capacitor is located in the middle of the dipole where surface currents are null for the dipole's 1.0-λ mode and maximum for 0.5- and 1.5-λ modes, such as to affect both the 0.5-/1.5-λ resonance least. By choosing proper values of the chip capacitor, the operating frequencies of the 1.0-λ mode, when port1 is excited, can be decreased to cancel out opposite-phased 0.5-λ mode on the opposite, half portion of the dipole close to port2, such that good isolation can be attained. Notice that these two resonances (0.5-/1.0-λ modes) are both required and combined for decoupling in this design; none of the resonances disappear. This is different from the working principle reported in [10].

Additionally, with the tuning stubs aiding in the dual-feed network, the desired frequency ratio of the 1.5- and 0.5-λ modes for the 5.2 GHz (5150–5350 MHz) and 2.4 GHz (2400–2484 MHz) bands can be obtained. Together with the 5.8 GHz resonance generated by parasitic strips in 0.25-λ monopole mode, a tri-band, 2.4/5.2/5.8-GHz wireless local area network (WLAN) operation is attained for the proposed dual-feed dipole antenna. Details of the dual-feed antenna system and the results thereof are described and discussed in the article.

2. PROPOSED, DUAL-FEED DIPOLE ANTENNA SYSTEM

2.1. Antenna Configuration and Design Consideration

Figure 1(a) illustrates the proposed, dual-feed antenna system affixed to the supporting metal plate of a 14-inch laptop display. In the experiments, the metal plate, made of stainless plate and coated with the zinc for solderability, measures 1 mm × 182 mm × 315 mm and can function as the large system ground for both the antennas and the electromagnetic interference (EMI) grounding. The proposed

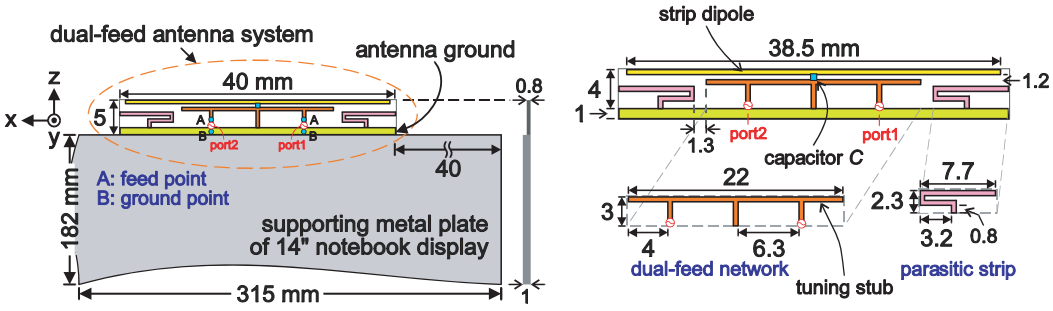

Figure 1. (a) Geometry of the dual-feed, dipole antenna for 2.4/5.2/5.8-GHz, tri-band WLAN operation affixed to the top edge of a display supporting plate. (b) Detailed dimensions of the design prototype.

design is constructed on the top side of a 0.8-mm-thick, flame retardant 4 (FR4) substrate ($\varepsilon_r = 4.4$ and loss tangent $\delta = 0.0245$) of size 5 mm × 40 mm and spaced 40 mm apart from the top-right corner of the metal plate. The top side of the substrate is flush with the top side of the display metal plate in the same x-z plane. The small antenna ground of size 1 mm × 40 mm is also reserved in the design footprint as it is used for practical applications for grounding the antenna system to the large system ground via a small copper tape (not shown here for brevity) in the assembly stage. Notice that owing to its low profile of 5 mm, the design is also well-suited to current narrow-bezel laptop computers [13–16].

The preferred parameters of the constructed prototype are detailed in Fig. 1(b). The design comprises a simple strip dipole of length 38.5 mm, a dual-feed network of compact size 3 mm × 22 mm, and two parasitic strips. The dipole is coupled-fed via a chip capacitor C connected to the feed network. Except for the antenna ground, all the strip widths are kept the same at 0.5 mm for ease of studies; the design structure is also symmetrically identical. At the beginning, the feed network looks like an inverted-E shape with port1 and port2 on the far ends and the shorting in the middle [see inset in Fig. 5(a)]. The strip dipole when fed by the dual-feed network is able to generate the fundamental (0.5-λ) and the two higher-order (1.0- and 1.5-λ) dipole modes. To obtain the desired frequency ratio of the 1.5- and 0.5-λ dipole modes for the 5.2 and 2.4 GHz bands, the tuning stubs of length 4 mm are incorporated in the dual-feed network. Then, the 5.8 GHz resonance is added by employing two parasitic strips in 0.25-λ monopole mode. Thereby, the tri-band WLAN operation is attained for the dual-feed dipole antenna.

The capacitor in this design controls the occurrence of the 1.0-λ dipole mode for each single port excitation at a time to be very close to the 0.5-λ dipole mode. When port1 is excited, the surface currents of the 1.0-λ dipole mode cancel out the opposite-phased currents of the 0.5-λ dipole mode on the opposite, half portion of the strip dipole, such that self-decoupled properties [9–12] around 2.45 GHz can be attained. It should be noticed that with only one feed port [see inset in Fig. 2(b)], the strip dipole only generates the 1.0-λ dipole mode. That's, the 0.5-λ dipole mode only occurs when the two feed ports are operating. More details regarding these two modes found on the same radiator (strip dipole) will be discussed in the following section. The preferred parameters in this paper were attained by rigorous studies simulated by the electromagnetic solver, ANSYS HFSS [17].

2.2. Decoupling Analyses and Controlling Mechanisms

Several reference cases are analyzed in this section to better understand the dual-feed antenna system and port decoupling. Fig. 2 shows the simulated S-parameters for the proposed design, reference case 1 (single feed port only), and reference case 2 (no capacitor C, replaced by direct-feed stub); all dimensions remain the same as those shown in Fig. 1. First, for the proposed design, three resonant modes (one in the lower band and two in the upper bands) with acceptable isolation (S_{21}) better than 15 and 12 dB in the 2.4 GHz (lower), and the 5.2/5.8 GHz (upper) bands respectively are seen in Fig. 2(a). For the cases of the single feed port only as depicted in reference case 1, the reflection coefficients (S_{11} for port1, S_{22} for port2) in Fig. 2(b) are very similar to their counterparts in Fig. 2(a). This suggests that each signal port in the proposed dual-feed antenna system suffers less coupling from the other port as the individual antenna with only port1 (Ant1) [or port2 (Ant2)] excitation in Fig. 2(b) functions independently.

However, when the capacitor is removed and replaced by a short stub [the strip dipole is direct-fed as shown in Fig. 2(c)], the isolation becomes worse, particularly in the lower band and the first upper band around 5.1 GHz, while the second upper band for 5.8 GHz operation is relatively less affected. This is because the fundamental (0.5-λ) and the second higher-order (1.5-λ) modes of the strip dipole mainly contribute to the 2.4 and 5.2 GHz bands while the two parasitic strips help generate the 5.8 GHz mode. And the loaded capacitor is employed to decouple the two feed ports of the same dipole resonance. Notice that the lower band for reference case 2 is also degenerated into two separate resonant modes at 2230 and 2450 MHz. The properties of these two modes are further elaborated with the aid of the surface current distribution in the following paragraph.

The surface-current distributions for port1 excitation for the proposed design and reference case 2 are presented in Fig. 3. The frequencies selected here represent the most matched frequency points studied in Fig. 2. The current null is denoted as a cross in the figure. First, for the proposed design, relatively large surface currents are seen populated on the half (right) portion of the design closer to port1 side as circled in Fig. 3(a). The 0.5-λ and 1.5-λ dipole mode currents with no null at 2450 MHz

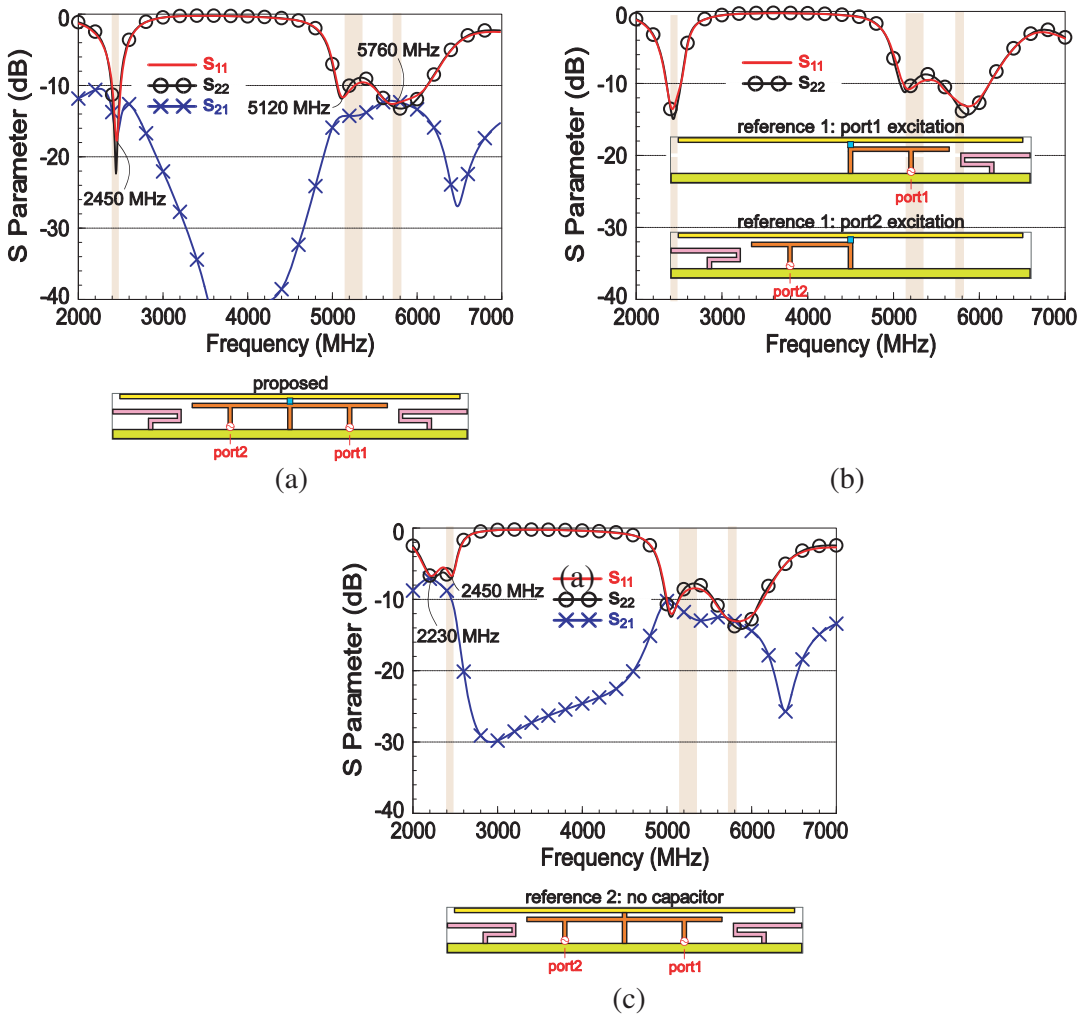

Figure 2. Simulated S parameters (S_{11} for port1, S_{22} for port2, S_{21} isolation between two ports) for (a) proposed design, (b) reference case 1 (port1 or port2 excitation only), and (c) reference case 2 (no capacitor C between dipole and dual-feed network); $C = 4.0$ pF.

and two nulls at 5120 MHz are also easy to identify. For reference case 2, the surface currents of the two different modes in the lower band as seen in Fig. 2(c) with 1.0-λ dipole mode at 2230 MHz and 0.5-λ dipole mode at 2450 MHz are seen in Fig. 3(b). The 1.0-λ dipole-mode current distributions on the strip dipole are similar to those for reference case 1 (port1 or port2 excitation only), and the frequencies thereof can be controlled (results not shown for brevity). From the previous studies in [12], larger capacitance leads to lower frequencies of the 1.0-λ dipole mode (monopole mode in [12]). And the direct-feed stub here resembles the case of using large values of the capacitor. Finally, the surface currents in the upper bands are about the same as those for the proposed design, but the isolation is not satisfactory as can been observed in Fig. 2(c).

The decoupling mechanisms are also illustrated in Fig. 3(c). The strip dipole can generate 0.5-, 1.0-, and 1.5-λ resonant modes. The center of the dipole, where the current null of the 1.0-λ mode occurs, is connected to the chip capacitor. When port1 is excited, the surface currents for 0.5- and 1.0-λ modes on the half (left) portion of the antenna close to port2 as circled in Fig. 3(c) are out of phases while in phase on the other (right) portion close to port1. This characteristic reflects those observed in Fig. 3(b). The frequencies of the 1.0-λ dipole mode can be controlled by the chip capacitor to be very close to the 0.5-λ dipole mode. As a result of the two resonant modes of similar magnitude but with opposite phases, the mutual coupling can be reduced [18].

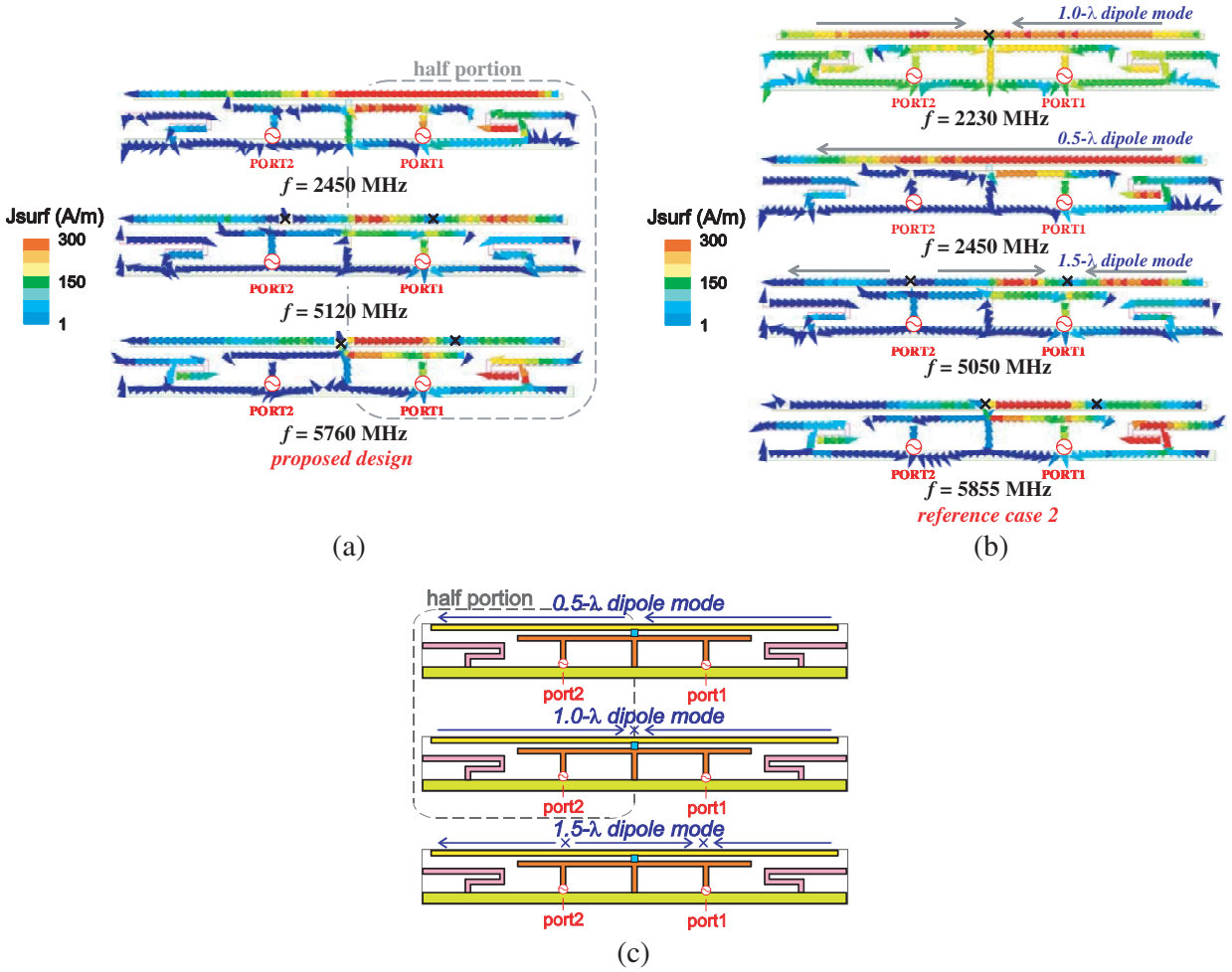

Figure 3. Simulated surface currents for port1 excitation at (a) 2450, 5120, and 5760 MHz for the proposed design and (b) 2230, 2450, 5050, and 5855 MHz for reference case 2. (c) Illustration of the decoupling mechanisms for the antenna in Fig. 3(b).

The port decoupling between the two ports in this design can be fine tuned by varying capacitor value C. Fig. 4 shows the simulated S parameters for the proposed design as a function of the capacitor C. The capacitor values are practically selected from the Murata GJM 0402 series datasheet. With the variation of 1 pF, the obtained S_{11} and S_{22} curves in Figs. 4(a) and (b) are comparatively unaffected; however, the S_{21} properties change quickly, especially in the 2.4 GHz band as seen in Fig. 4(c). The drop (smallest value) of the S_{21} varies from -15.4 dB at 2.43 GHz ($C = 3$ pF) to -20.6 dB at 2.50 GHz ($C = 5$ pF). The near-optimum value of the capacitor in this study is 4 pF, which gives a S_{21} drop of -17 dB around 2.45 GHz.

Figure 5 further explains how the dual-feed dipole system evolves with regard to the tri-band operation for each 2.4, 5.2, and 5.8 GHz band. At the beginning, the strip dipole is connected, via the chip capacitor, to the inverted-E-shaped dual-feed network as shown in the inset of reference case 3 in Fig. 5(a). The tuning stubs are not yet incorporated in the dual-feed network, and the length of the dipole is extended at both ends by 3 mm to operate in the 2.4 GHz band. It can be seen that the fundamental (0.5-λ) and the second higher-order (1.5-λ) dipole modes resonate at 2.45 and 6.56 GHz, respectively. The S parameters in the lower band are comparable to those of the proposed design (see corresponding dashed lines). To lower the 1.5-λ dipole mode for operating in the 5.2 GHz band, the tuning stubs of 5.3 mm are added to the feed network as shown in the inset in Fig. 5(b). In this case, the single strip dipole can generate at the 2.4 and 5.2 GHz bands with isolation (S_{21}) better than 16 and

14 dB, respectively. By further applying two parasitic strips to reference case 4, the tri-band, dual-feed dipole antenna system can be attained. Notice that for the proposed design, the operating frequencies of the two parasitic strips are decoupled by the large distance therein between (24.6 mm, about 0.47λ at 5725 MHz).

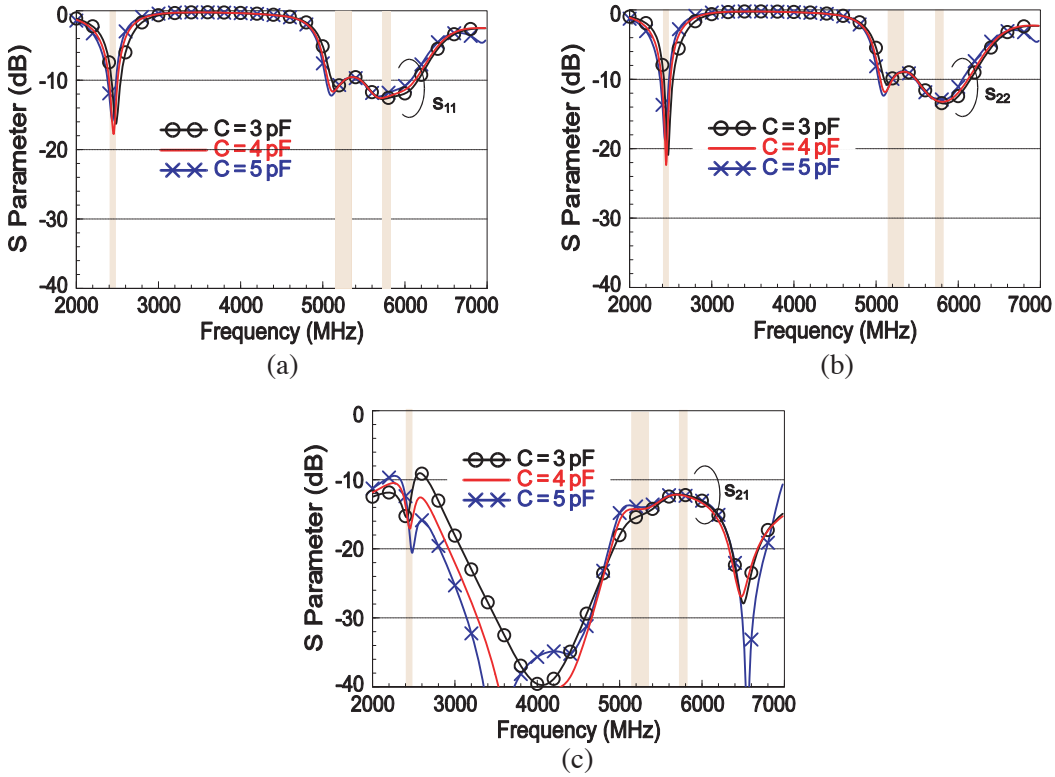

Figure 4. Simulated S parameters for the proposed design as a function of the capacitor C: (a) S_{11} for port1, (b) S_{22} for port2, and (c) S_{21} isolation between two port excitation.

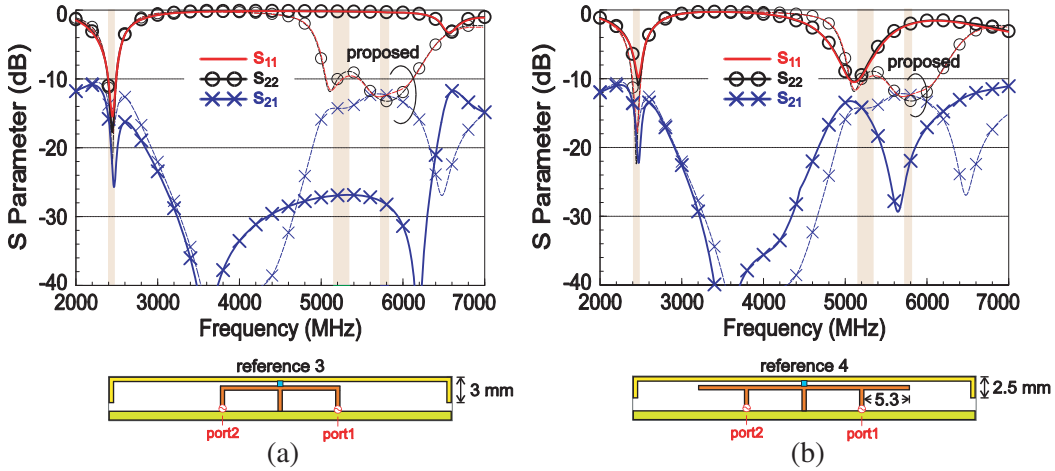

Figure 5. Simulated S parameters for (a) reference case 3 (proposed without tuning stubs and parasitic strips) and (b) reference case 4 (proposed without parasitic strips); all dimensions remain the same except for those indicated in insets.

3. EXPERIMENTAL AND SIMULATION RESULTS

Figure 6 shows the measured and simulated S-parameters for the proposed dual-feed dipole antenna system. The simulation results are presented by dashed lines. The targeted 2.4 and 5.2/5.8 GHz WLAN bands are marked by the three shaded frequency ranges. The experimental data in general agree with the simulation. The reflection coefficients (S_{11} and S_{22}) within the bands of interest are all below -7.4 dB (about VSWR of 2.5), which is industrially acceptable for WLAN laptop antennas and corresponds to about 0.8 dB transmission loss via the antenna. The measured isolation (S_{21}) between the antennas over the 2.4 and 5.2/5.8 GHz bands is better than 16 and 14 dB. The two 50-Ω mini-coaxial cables of length about 80 mm are used for feeding the dual-feed network across a feed gap of 0.5 mm. The inner conductor of the cable is connected to point A while the outer grounding is soldered to point B on the small antenna ground (see points A and B in Fig. 1).

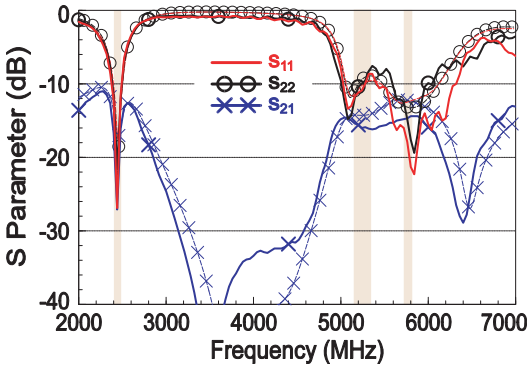

Figure 6. Measured and simulated (gray dash lines) S parameters for the proposed design; $C = 4.0$ pF.

The radiation performance of the constructed prototype was measured at our in-house SATIMO chamber of model SG 64, which has multiple probe arrays and uses the conical-cut method [19]. Figs. 7 and 8 show the measured radiation patterns in E_θ and E_φ fields for port1 and port2 excitation, respectively, at 2442, 5250, and 5775 MHz, the center frequencies of the 2.4, 5.2, and 5.8 GHz bands. During the measurement for port1 excitation, port2 was terminated at the 50-Ω load connector, and vice versa. Across the bands, comparable E_θ and E_ϕ fields are observed in the x-y planes, which is advantageous to WLAN operation in complex propagation environments. Also, similar to the radiation properties of the WLAN laptop antenna as studied in [15], the radiation patterns in the two major elevation planes (x-z and y-z planes) show larger radiation above the display toward the $+z$ direction.

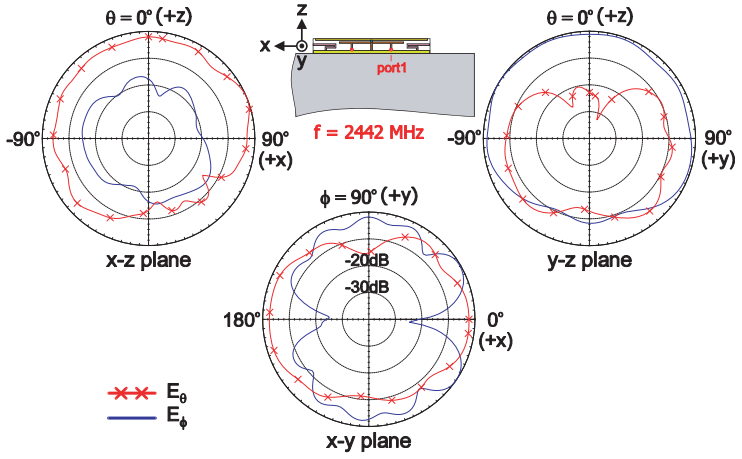

(a)

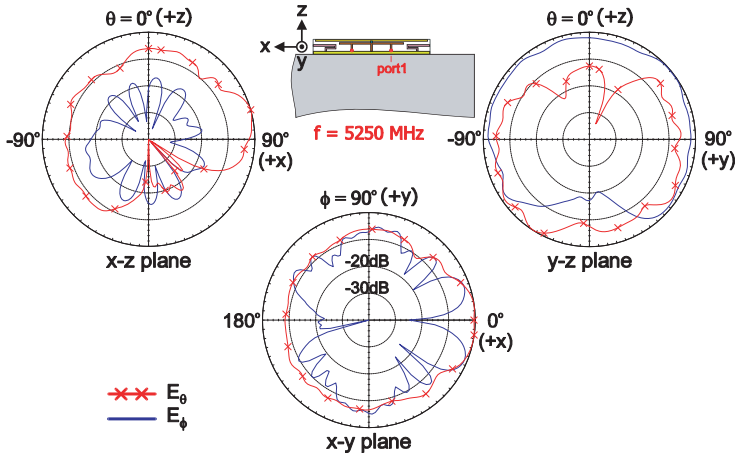

(b)

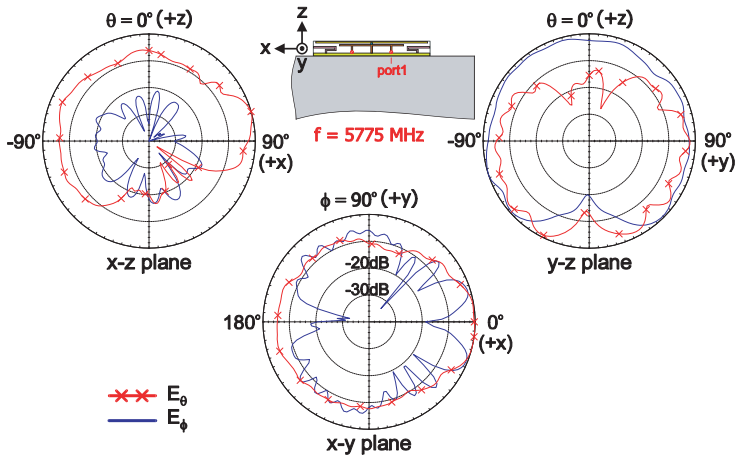

(c)

Figure 7. Measured 2D radiation patterns for port2 excitation in the proposed design at (a) 2442 MHz, (b) 5250 MHz, and (b) 5775 MHz.

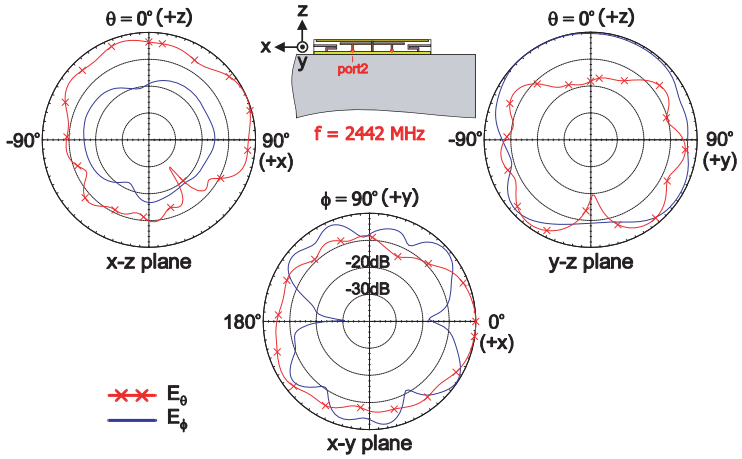

(a)

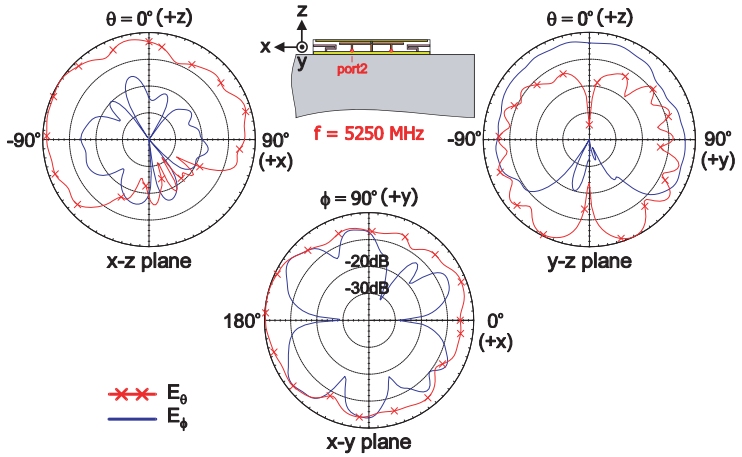

(b)

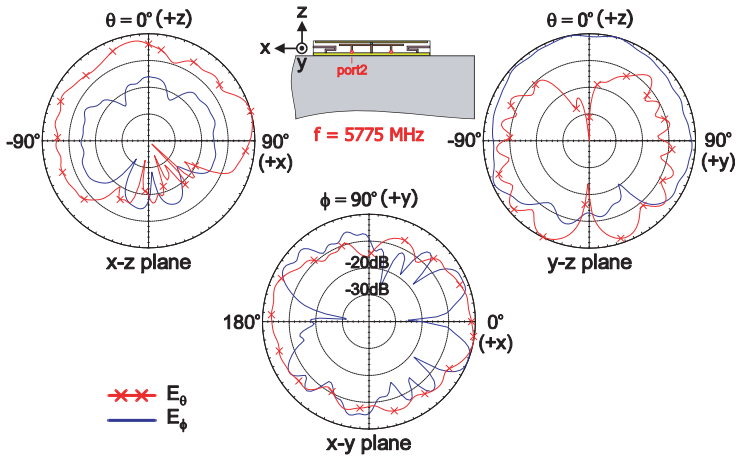

(c)

Figure 8. Measured 2D radiation patterns for port1 excitation in the proposed design at (a) 2442 MHz, (b) 5250 MHz, and (b) 5775 MHz.

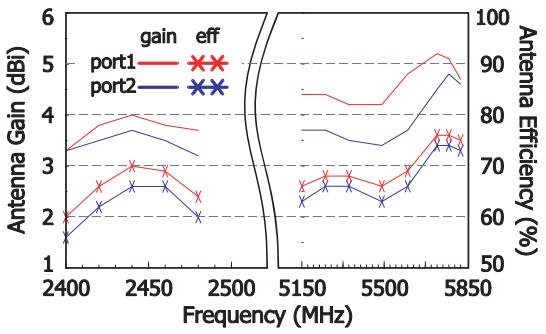

Figure 9. Measured peak antenna gain and antenna efficiency for port1 and port2 excitation studied in Figs. 7 and 8.

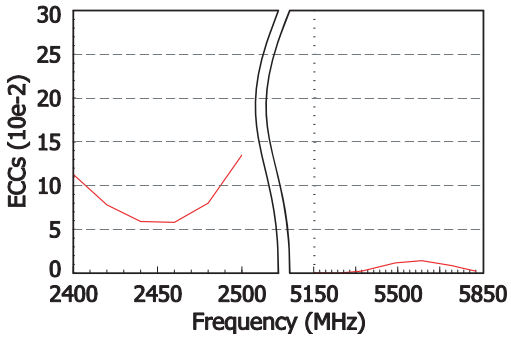

Figure 10. Simulated ECC based on the simulated, complex, E-field radiation patterns for port1 and port2 excitation studied in Fig. 6.

Figure 9 plots the measured peak antenna gain and antenna efficiency against frequency. For port1 excitation of the proposed design in the 2.4 and 5.2/5.8 GHz bands, the peak gain is about 3.3–4.0 and 4.1–5.1 dBi with antenna efficiency larger than 60% and 66%, respectively. As for port2 excitation,

the gain is about 3.2–3.7 and 3.5–4.9 dBi with efficiency larger than 57% and 63% in the lower and the two upper bands. The radiation measurement here took account of the antenna mismatch and the mini-coaxial cable loss. The realized gain [20] and the antenna efficiency [21] were measured in the chamber.

The envelope correlation coefficient (ECC) for the dual-feed antenna system is given in Fig. 10. The ECC is also obtained from the ANSYS HFSS, which computes the Hermitian product of the two far-field 3D radiation patterns with each normalization [22]. Very good ECC smaller than 0.06 and nearly zero are obtained over the 2.4 and 5 GHz bands, respectively, which are much better than the value 0.5 as suggested for mobile devices reported in [23].

4. CONCLUSION

A single strip dipole fed by a dual-feed network via a chip capacitor for achieving a dual-feed antenna system for 2.4/5.2/5.8-GHz WLAN operation has been proposed. The strip dipole generates in both the 0.5-λ and 1.5-λ dipole modes to cover the 2.4 and 5.2 GHz bands. The 5.8 GHz band is contributed to by the 0.25λ monopole mode of the added parasitic strips. A chip capacitor is loaded between the strip dipole and the dual-feed network to enhance the two-port isolation of the dipole antenna. The capacitor is used to decrease the operating frequencies of the 1.0-λ dipole mode for each single port excitation to cancel out opposite-phased 0.5-λ dipole-mode currents on the strip dipole when the dual-feed network is operating, such that good isolation can be attained. The measured port isolation is better than 16 and 14 dB over the 2.4 and 5.2/5.8 GHz bands. The antenna efficiency overall exceeds about 60% across the bands. The proposed design is simple in structure and compact in size, very promising for future multiple laptop antennas for Gbps communications.

REFERENCES

1. CNET, "5G laptops are coming this year. Here's the first batch from CES 2020," https://www.cnet.com/news/5g-laptops-coming-this-year-first-batch-ces-2020/.
2. Kang, T. W. and K. L. Wong, "Isolation improvement of 2.4/5.2/5.8 GHz WLAN internal laptop computer antennas using dual-band strip resonator as a wavetrap," *Microw. Opt. Technol. Lett.*, Vol. 52, 58–64, 2010.
3. Guo, L., Y. Wang, Z. Du, Y. Gao, and D. Shi, "A compact uniplanar printed dual-antenna operating at the 2.4/5.2/5.8 GHz WLAN bands for laptop computers," *IEEE Antennas Wireless Propagat. Lett.*, Vol. 13, 229–232, 2014.
4. Liu, Y., Y. Wang, and Z. Du, "A broadband dual-antenna system operating at the WLAN/WiMax bands for laptop computers," *IEEE Antennas Wireless Propagat. Lett.*, Vol. 14, 1060–1063, 2015.
5. Deng, J. Y., J. Y. Li, L. Zhao, and L. X. Guo, "A dual-band inverted-F MIMO antenna with enhanced isolation for WLAN applications," *IEEE Antennas Wireless Propagat. Lett.*, Vol. 16, 2270–2273, 2017.
6. Su, S.-W. and Y. W. Hsiao, "Small-sized, decoupled two-monopole antenna system using the same monopole as decoupling structure," *Microw. Opt. Technol. Lett.*, Vol. 61, 2049–2055, 2019.
7. Su, S.-W., C. T. Lee, and Y. W. Hsiao, "Compact two-inverted-F-antenna system with highly integrated π-shaped decoupling structure," *IEEE Trans. Antennas Propagat.*, Vol. 67, 6182–6186, 2019.
8. Wan, C.-C. and S.-W. Su, "Compact, self-isolated 2.4/5-GHz WLAN antenna for notebook computer applications," *Progress In Electromagnetics Research M*, Vol. 83, 1–8, 2019.
9. Wong, K. L., C. Y. Tsai, and J. Y. Lu, "Two asymmetrically mirrored gap-coupled loop antennas as a compact building block for eight-antenna MIMO array in the future smartphone," *IEEE Trans. Antennas Propagat.*, Vol. 65, 1765–1778, 2017.
10. Ren, Z. and A. Zhao, "Dual-band MIMO antenna with compact self-decoupled antenna pairs for 5G mobile applications," *IEEE Access*, Vol. 7, 82288–82296, 2019.

11. Wong, K. L., B. W. Lin, and S. E. Lin, "High-isolation conjoined loop multi-input multi-output antennas for the 5G tablet device," *Microw. Opt. Technol. Lett.*, Vol. 61, 111–119, 2019.
12. Wan, C.-C. and S.-W. Su, "Conjoined, 2.4/5-GHz WLAN two-monopole system decoupled using mode-controlled capacitor for notebook computers," *Progress In Electromagnetics Research M*, Vol. 87, 1–10, 2019.
13. Su, S.-W., C. T. Lee, and S. C. Chen, "Compact, printed, tri-band loop antenna with capacitively-driven feed and end-loaded inductor for notebook computers," *IEEE Access*, Vol. 6, 6692–6699, 2018.
14. Su, S.-W., "Capacitor-inductor-loaded, small-sized loop antenna for WLAN notebook computers," *Progress In Electromagnetics Research M*, Vol. 71, 179–188, 2018.
15. Su, S.-W., "Very-low-profile, 2.4/5-GHz WLAN monopole antenna for large screen-to-body-ratio notebook computers," *Microw. Opt. Technol. Lett.*, Vol. 60, 1313–1318, 2018.
16. Su, S.-W., "Very-low-profile, small-sized, printed monopole antenna for WLAN notebook computer applications," *Progress In Electromagnetics Research Letters*, Vol. 82, 51–57, 2019.
17. ANSYS HFSS, ANSYS Inc., http://www.ansys.com/Products/Electronics/ANSYS-HFSS.
18. Li, M., L. Jiang, and K. L. Yeung, "Novel and efficient parasitic decoupling network for closely coupled antennas," *IEEE Trans. Antennas Propag.*, Vol. 67, 3574–3585, 2019.
19. SG 64, MVG, https://www.mvg-world.com/en/products/antenna-measurement/multi-probe-systems/sg-64.
20. Volakis, J. L., *Antenna Engineering Handbook*, 4th edition, Chapter 6, 16–19, McGraw-Hill, New York, 2007.
21. Balanis, C. A., *Antenna Theory: Analysis and Design*, 3rd edition, Chapter 2, Wiley, Hoboken, NJ, 2012.
22. Blanch, S., J. Romeu, and I. Corbella, "Exact representation of antenna system diversity performance from input parameter description," *Electronics Lett.*, Vol. 39, 705–707, 2003.
23. Vaughan, R. G. and J. B. Andersen, "Antenna diversity in mobile communications," *IEEE Trans. Vehicular Technol.*, Vol. 36, 149–172, 1987.